Engineered axon tracts within tubular biohybrid scaffolds

Laura Rodríguez Doblado[1], Cristina Martínez-Ramos[1,2], José Manuel García-Verdugo[3], Victoria Moreno-Manzano[4,5] and Manuel Monleón Pradas[1,6,*]

[1]*Center for Biomaterials and Tissue Engineering, Universitat Politècnica de València, Spain*

[2] *Department of Medicine, Universitat Jaume I, Av. Vicent-Sos Baynat s/n, Castellón 12071, Spain.*

[3] *Laboratory of Comparative Neurobiology, Instituto Cavanilles, Universitat de València, CIBERNED, Spain*

[4] *Neuronal and Tissue Regeneration Lab, Centro de Investigación Príncipe Felipe, Valencia, Spain*

[5]*Universidad Católica de Valencia, Valencia, Spain*

[6]*Networking Research Center on Bioengineering, Biomaterials and Nanomedicine (CIBER-BBN), Spain*

** Corresponding author. E-mail address:* Manuel Monleón Pradas, PhD. Phone: +34 963877277 E-mail: mmonleon@ter.upv.es

Abstract

Injuries to the nervous system that involve the disruption of axonal pathways are devastating to the individual and require specific tissue engineering strategies. Here we analyse a cells-biomaterials strategy to overcome the obstacles limiting axon regeneration *in vivo*, based on the combination of a hyaluronic acid (HA) single-channel tubular conduit filled with poly-L-lactide acid (PLA) fibres in its lumen, with pre-cultured Schwann cells (SC) as cells supportive of axon extension. The HA conduit and PLA fibres sustain the proliferation of SC, which enhance axon growth acting as a feeder layer and growth factor pumps. The parallel unidirectional ensemble formed by PLA fibres and SC tries to recapitulate the directional features of axonal pathways in the nervous system. A dorsal root ganglion (DRG) explant is planted on one of the conduit's ends to follow axon outgrowth from the DRG. After a 21-day co-culture of the DRG+SC-seeded conduit ensemble, we analyse the axonal extension throughout the conduit by scanning, transmission electronic and confocal microscopy, in order to study the features of SC and the grown axons and their association. The separate effects of SC and PLA fibres on the axon growth are also experimentally addressed. The biohybrid thus produced may be considered a synthetic axonal pathway, and the results could be of use in strategies for the regeneration of axonal tracts.

Keywords: axon tract, hyaluronic acid conduit, poly-lactic fibres, dorsal root ganglion cell culture, Schwann cell culture

1. Introduction

Axon regeneration in the central nervous system (CNS) is severely restricted after traumatic brain injury, stroke, spinal cord injury (SCI) and related conditions that involve axonal disruption. In contrast, peripheral nervous system (PNS) axons can regenerate in some cases allowing functional recovery when the damage involves a relatively short distance [1,2]. After damage, CNS axons have an intrinsically limited capability to regenerate and they are surrounded by a local inhibitory environment [3]. Moreover, the loss of neuronal populations and synaptic connections is most irreversible due to the limited outgrowth capacity of mature neurons [4].

In axonal pathways, the axons form parallel bundles (in nerves in the PNS, in tracts in the CNS). Therefore, approaches that facilitate axonal guidance are sought for the regeneration of axonal pathways, both in the PNS and the CNS. Strategies for promoting axon guided growth *in vivo* after injury include reversing the inhibitory stimuli for axon growth [5], increasing intrinsic neural regenerative programs [6], providing a substrate to guide axon growth [7], adding neural elements facilitating axon growth [8], and cell transplantations. Cells transplants, in most cases, are limited to local effects on the host's circuits without rebuilding the damage. For instance, numerous attempts have been made to integrate various types of cells after SCI, like neural stem/progenitor cells [9], oligodendrocyte progenitor cells [10] or Schwann cells (SC) [11][12]. Transplantation approach has mostly shown poor or null ability to rebuild damaged circuits and reinstating the cytoarchitecture of damaged or lost CNS tracts [13]. However, Kumamaru and collaborators recently showed that grafted foetal NPCs into the injured spinal cord adopt certain sensory and motor spinal interneuron fate, which innervate to growing host damaged corticospinal tract recapitulating motor domains without the need of additional exogenous guidance [14].

SC play an important role in neuroregeneration and protection in the PNS [15,16] and are responsible for the myelination of axons. After injury, SC activate, divide, de-differentiate and proliferate distally contributing to nerve repair [17]. SC are a source of neurotrophic, angiogenic factors, and surface proteins that are involved in the maintenance of normal nervous system function and the activation of an innate immune response after injury [18], Their regenerative potential when transplanted in the CNS has also been assessed [11,12,19]; after a phase I clinical trial, SC transplantation proved to be safe, and there were no adverse effects due to the transplants, the surgery, or the methods used for cell delivery. For these reasons, use of SC has been proposed for regenerative purposes both in the PNS [20,21] and the CNS [22,23].

Tissue engineering approaches employing biomaterials emerged in order to improve over the limitations of purely cell-based therapies. These approaches propose the combination of natural or artificial nerve guidance conduits with cell transplantation and/or growth factor delivery to facilitate guiding axonal regrowth [24]. A nerve conduit should provide a suitable environment for neuron survival and axonal extension, guide axonal projections, and mimic the biomechanics with adequate mechanical properties [25]. Use of biocompatible scaffolds represents a benefit when used as a vehicle with minimal tissue invasiveness in comparison with intra-parenchymal transplantation approaches, conferring protection of the transplanted cells against the hostile environment generated at the injury site [26].

Two different types of biomaterials were employed in the conduit scaffolds here proposed: a HA hollow conduit and poly-L-lactide acid (PLA) microfibers in their lumen [27,28]. HA is a hydrogel with good biocompatibility, biodegradability, and therapeutic benefits on neuronal regeneration processes [29], and exhibits mechanical properties similar to soft nervous tissues [30]. As previously shown [27,28], SC seeded into crosslinked HA conducts with suitable diameters and wall pore structure filled

with PLA fibres were able to proliferate and self-organize into a continuous cylindrical cell sheath spanning the whole distance of the conduit and cover the fibres [27]. The present study builds on this finding exploiting the thus-produced SC structure as a feeder layer for directed axon growth. PLA is a synthetic polyester with a long history as a biomedical material due to its outstanding mechanical properties, biocompatibility [31], and biodegradability [32]. PLA fibres raised interest as part of the tubular conduit concept when allocated in the lumen [33,34] providing a support for cell adhesion, migration and elongation in a guided way. As previously shown [35] HA conduits filled with PLA fibres induced preferential neuronal differentiation of progenitor cells *in vitro* and showed total biocompatibility and beneficial effects *in vivo* in a SCI model. Smaller fibre diameters have shown better guided axonal growth effects than larger diameter [36], and in our study we opted to employ PLA fibres of 30 μm diameter.

The present study combines a nerve guidance conduit with supportive cells to overcome the typical limitations of axon regeneration, and establishes an experimental model to follow axon growth in vitro within the developed construct. A sequential methodology was used:: first, we establish a SC culture within our HA-PLA conduit for a number of days, and then we plant a dorsal root ganglion (DRG) explant at one end of the conduitas a source of projecting neurons, thus locating the neurons at a single point and recapitulating the in vivo situation of a lesion to some aspects. With the first SC culture, a feeder-like structure is formed by the SC on the PLA fibres. Thus, when we cultured the DRG explant on one end of the conduit, the growth of sprouting axons doesn't have to wait for migrating SC from the DRG explants, and this improves the velocity axonal growth, also enhanced by the growth factors released by the pre-seeded SC in the HA-PLA conduit. Axon extension from the DRG explant into the SC-seeded conduit was then followed in time and characterized. We investigated the effects on the axon growth of the presence or absence of the SC and the PLA microfibers in the HA tubular

scaffolds. This biohybrid construct proved effective in promoting directed axon growth, and the results may thus be of interest for the goal of reconstructing axonal tracts.

2. Materials and methods

2.1. Cell source

Primary rat SC (P10301, Innoprot) expanded with SC Medium (P60123, Innoprot) were employed at 4-5 cell passage for cell cultures in the materials. Sprague–Dawley rats from Charles River and SD-Tg(GFP)2BalRrrc from Rat Resource & Research Center (University of Missouri Columbia, Columbia, MO, USA) were used for DRG explants dissection and were maintained following the National Guide to the Care and Use of Experimental Animals (Real Decreto 1201/2005). After the sacrifice by decapitation, whole DRG or DRG-GFP explants were dissected from the spinal column of neonatal rats (P3-P4) and transferred into ice-cooled Dulbecco's modified Eagle medium (DMEM; 11965118, Thermo Fisher Scientific) containing 10% foetal bovine serum (FBS; 26140, Thermo Fisher Scientific), using a dissecting microscope to remove the remaining nerves and connective tissue.

2.2. Preparation of hyaluronic acid conduits and hyaluronic acid conduit with poly-L-lactic acid fibres

The synthesis of HA from *Streptococcus equi* (HA; 1.5–1.8 MDa, 53747, Sigma-Aldrich) conduits was carried out as previously described [27,28]. Briefly, poly-ε-caprolactone (PCL, 19561, PolySciences) fibres of 400 μm were extruded in Hater Minilab and a polytetrafluoroethylene thin block with 1.5 mm-wide grooves with a single PCL fibre of 400 μm diameter was used as a mould for the conduits. 5% (w/v) of HA was dissolved for 24 h in sodium hydroxide 0.2 M (SO0420, Scharlab). Then, the HA was crosslinked with divinyl sulfone (DVS; V3700, Sigma-Aldrich) in a 9:10

DVS:HA monomeric units molar ratio, and this solution was mixed and injected in a mould. Later, the solution in the mould was lyophilised for 24 h (Lyoquest-85, Telstar). Finally, the conduits were hydrated in distilled water, the PCL fibres were extracted, and the conduits with a 400 µm inner diameter, were cut to 6 mm length (HA hereafter). In several conduits, 20 aligned PLA fibres of 30 µm diameter and 10 mm length (AITEX Textile Research Institute, Spain) were placed inside the lumen of the 6 mm length conduits with the help of a needle, as a loose bundle of individual fibres. The group constituted of conduit and PLA fibres inside was named HAf hereafter. Before the seeding of the cells, the conduits were sanitised for 2h with 70º ethanol (ET0002, Scharlab), then conduits were immersed in 50º, 30º ethanol and distilled water for 10 min, in order to prepare them for the culture and to eliminate the non-crosslinked DVS to avoid the cytotoxicity of the unreacted residues. Finally, conduits were conditioned overnight with culture medium (DMEM containing 10% FBS).

2.3. Cell culture and cell seeding within conduits

SC (P10301, Innoprot, Spain) (4-5 cell passage were grown in flasks until confluence at 37ºC, 5% CO_2, in SC medium (P60123, Innoprot, Spain). SC were seeded at a density of $1x10^5$ cells/conduit suspended in 3 µl of SC medium with Hamilton syringe (26236, SGE Analytical Science), inserting the syringe at one end on the conduit, both in HA and HAf groups. After 10 days of SC culture, DRG explants were placed in direct contact with one end of the conduit and were then transferred into 48-well plates, which was maintained with a specific DRG medium (Neurobasal medium, 21103049; D-glucose 2mg/mL, G7021; L-glutamine 100X, 25030-024; 1% FBS; 1% penicillin/streptomycin, 15140122; 2% B27 supplement, 17504044; 0,1% NGF, 13257019 (Thermo Fisher Scientific)) refreshed every 2 days until 21 additional days counted from the moment the DRG was seeded. When indicated, in some experiments

DRG-GFP explant were employed. In order to assess the different effect of the different components of the construct, four different experimental groups were established: (1) HA conduit with the DRG explant (named as HA+DRG), (2) the HA conduit with the 20 PLA fibres inside (HAf) with the DRG explant (HAf+DRG), (3) the HA conduit seeded with SC (HA+SC) with the DRG explant (HA+SC+DRG), and (4) the HA conduit with the 20 PLA fibres inside seeded with SC (HAf+SC) with the DRG explant (HAf+SC+DRG). A schematic representation of the working groups is shown below (figure 1).

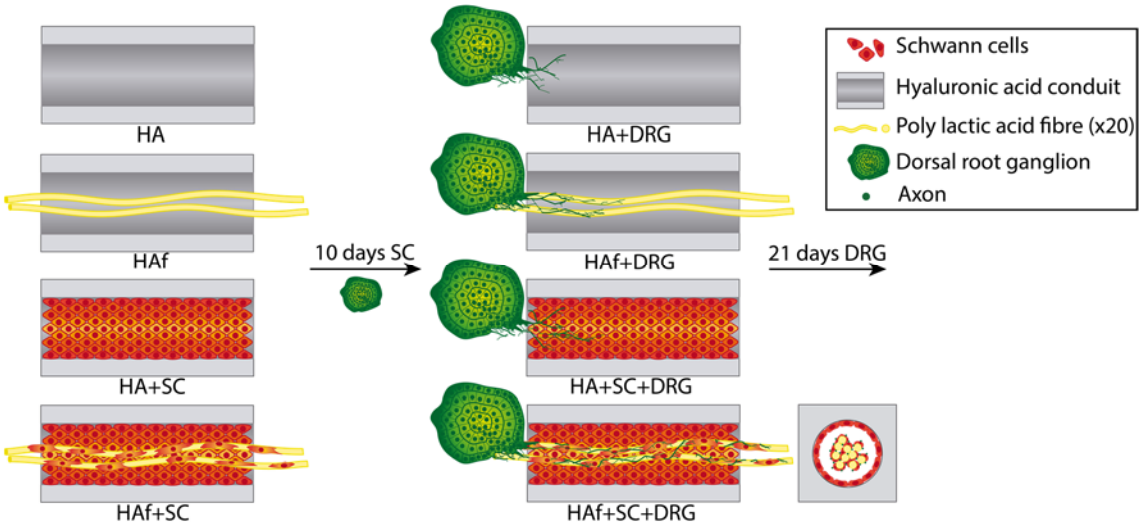

Figure 1. Experimental setup. Schematic cross-section representation of the different experimental groups employed in work. In the groups with SC, SC were seeded and maintained in the conduits for 10 days before the planting of the DRG, which was then cultured for another 21 days. In the left, groups before the seeding of DRG explant (HA, HAf, HA+SC, HAf+SC). In the right, groups after the seeding of the DRG explant (HA+DRG, HAf+DRG, HA+SC+DRG, HAf+SC+DRG). All groups were analysed at the experimental day 21 after DRG seeding.

2.4. Scanning (SEM) and Transmission electron microscopy (TEM)

After culture, samples for SEM were washed in Phosphate Buffer Saline (PBS) 0.1M and fixed in 3.5% glutaraldehyde (GA; 16210, Electron Microscopy Sciences) solution for 1h at 37ºC, post-fixed with 2% OsO4 (Electron Microscopy Sciences) and dehydrated. Later, conduits were processed in a critical point dryer (critical point values: 328C, 1100 psi). The conduits were cut longitudinally to expose their internal lumina and coated with an ultrathin layer of gold and observed at an acceleration tension of 10 kV in a scanning electron microscope (Hitachi S-4800, EE.UU.). Regarding TEM, samples were washed in PBS 0.1M and fixed in 2% paraformaldehyde (PFA; 47608, Sigma-Aldrich)-2.5% GA solution for 5h at 37ºC, post-fixed with 2% OsO_4 (19100-19134, Aname) and dehydrated in a series of ethanol solutions of increasing concentration. Later, conduits were stained with 2% uranyl acetate (22400, Electron Microscopy Sciences), embedded in araldite resin (A3183, Sigma-Aldrich) and allowed to solidify at 70ºC for 72h. The conduits embedded in araldite resin were cut crosswise in semithin sections (1.5 μm), stained with 1% toluidine blue (89640, Sigma-Aldrich) and sections of interest were detached from the glass-slides by repeated freezing and thawing in liquid N_2. Selected sections were further sectioned with and ultramicrotome (Leica EM UC6, Leica, Spain) to obtain ultrathin sections (50-60 nm). The proximal, medium, and distal part of each conduit were visualised and studied with a transmission electron microscope (FEI Tecnai Spirit G2, EE.UU.). Quantification of the number of axons at the proximal and distal part of HAf+SC+DRG was performed employing representative TEM images with a common area.

2.5. Staining and immunocytochemistry

SC seeded for 10 days were characterised with by Coomassie staining. The samples were rinsed with PBS 0.1M and fixed in 4% PFA for 20 min. The cells were then stained in a 0.2% solution of Coomassie brilliant blue R250 (1125530025, Sigma-

Aldrich) in methanol:acetic acid:distilled water, 46.5:7:46.5 (v/v/v) (320390, A6283, Sigma-Aldrich) for 1h and rinsed several times in distilled water. The structure formed by the SC inside the lumen were extracted cutting the conduits and images were acquired with a Nikon Eclipse i80 microscope (EE.UU.). Glial and neural population and neurite outgrowth were identified analysing the expression of different markers by immunofluorescence with confocal laser scanning microscopy: neuron-specific class III β-tubulin (Tuj1; neurons), myelin basic protein antibody (MBP; glial cells and myelin membrane), S100 calcium-binding protein antibody (S100; glial cells), growth associated protein 43 (GAP43; growth cones), p75 NGF receptor antibody (p75; glial marker), and neurofilament heavy polypeptide antibody (NF; neurons). For confocal microscopy, the conduits were rinsed thoroughly with PBS 0.1M and fixed in 4% PFA for 20 min. Cells were permeabilised and blocked with 0.1% Triton X-100 (T8787, Sigma-Aldrich), 10% FBS in PBS 0.1M for 2h. Conduits were then incubated at 4°C overnight with primary antibodies in PBS 0.1M with 0.1% Triton X-100 and 10% FBS: mouse monoclonal TuJ1 (1/300; MO15013, Neuromics) and MBP (1/400; ab62631, Abcam); rabbit monoclonal GAP43 (1/400; ab75810, Abcam) and p75 (1/200; ab52987, Abcam); and rabbit polyclonal NF (1/800; ab8135, Abcam) and S100 (1/200; S2644, Sigma-Aldrich). Secondary antibodies, goat anti-mouse IgG Alexa Fluor® 488 and 633 and goat anti-rabbit IgG Alexa Fluor® 488 and 633, and ActinRed™ 555 ReadyProbes™ Reagent (2 drops/ml; Thermo Fisher), in PBS 0.1M with 0.1% Triton X-100 and 10% FBS were used for a further 2 hours of incubation at room temperature in the darkness at 1/200 (A28175, A-21052, A-11008, A-21070; Thermo Fisher Scientific, respectively). Afterwards, samples were incubated with DAPI in PBS 0.1M (1/5000; D9564, Sigma-Aldrich) during 10 min to stain nuclei. As a negative control, there was no primary antibody in the reaction before the secondary antibody was added. Previous published studies employ specific SC and DRGs markers, and the most

commonly used are MBP [37,38], p75 [37,39], S100 [40,41], GAP43 [42,43], NF [44,45], and III β-tubulin [35,46]. It was necessary to make a longitudinal cut of the conduits before performing the immunocytochemistry assay to obtain a complete view of the lumen before using a confocal microscope (LEICA TCS SP5, Leica microsystems, Spain). In some samples, it was necessary to take off the PLA fibres to take images of the whole length of the PLA fibres after removing the HA conduits. The confocal images were processed with an overlay to make a reconstruction of the total length of the conduits. Neurite length on conduit and fibres were measured in the reconstruction of the confocal fluorescent images using Image J software (using three independent replicates (n=3) of each studied group).

2.6. Statistical analyses

Each experiment was performed at least four times unless otherwise noted. For all the experiments, three independent replicates (n=3) of each studied group were employed. Data were expressed as mean ± standard deviation (SD). The Shapiro-Wilk test was used to confirm the data normality on GraphPad Prism 8. Results were analysed by t-student test on normal data and Mann-Whitney test in the opposite case. A 95% confidence level was considered significant. An asterisk * indicates statistically significant differences, indicating a p-value below 0.05.

3. Results

3.1. Schwann cells seeded inside the lumen of hyaluronic acid conduits generate an internal Schwann cell sheath

We seeded rat SC in the lumen of the conduit and cultured them for 10 days (figure 2). The SC formed a tight cell mantle with a consistency that kept them together so that it could easily be detached from the channel's surface and taken outside, as seen in the

figure 2(a), stained in blue with Coomassie. The consistency of this SC sheath structure allows its folding without breaking, as can be seen on figure 2(a), where the more intensely coloured regions correspond to overlapped crimped parts of the length of the cell cylinder. The SC cylindrical sheath-like tapestry spans continuously to the whole length of the internal lumen (figure 2(b), blue), composed by several layers of cells that contact tightly. These cells presented elongated nuclei, lax chromatin, and homogeneously distributed organelles in their cytoplasm (figure 2(c)). These cells also presented notable cell contacts which were particularly strong compared to surrounding areas. Although these were not typical junctional complexes, a thickened cell membrane could be observed due to higher density of electron-dense material (supplementary figure 1).

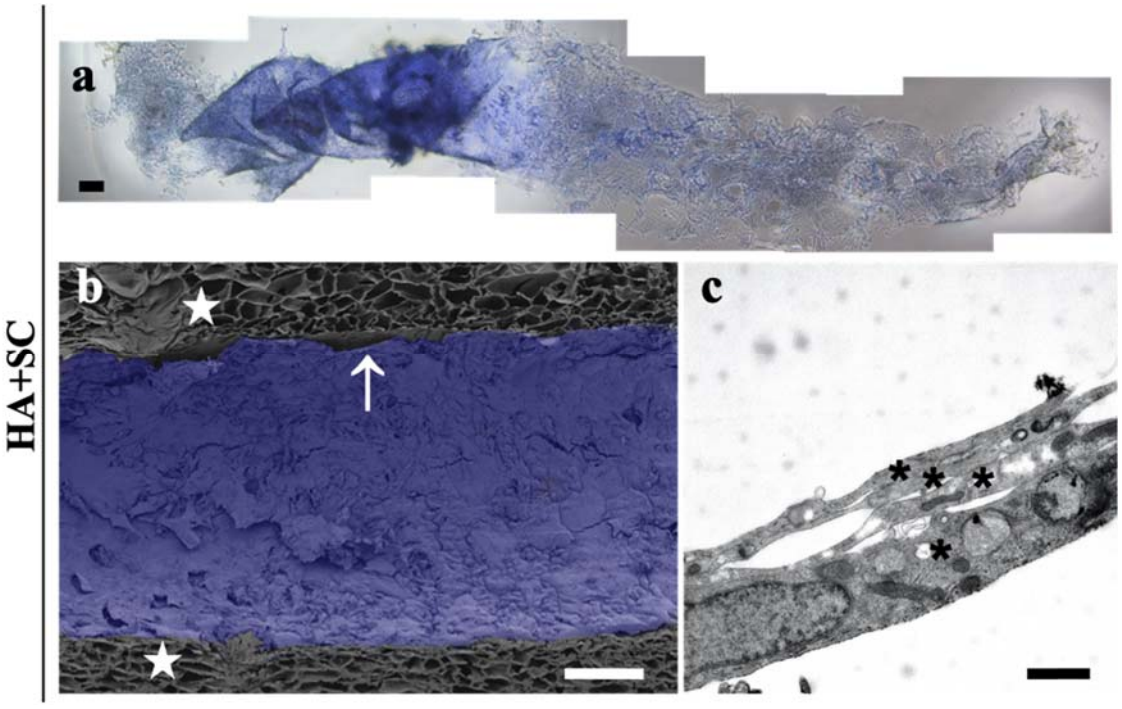

Figure 2. Schwann cells grown inside the hyaluronic acid conduits. (a) Bright field photograph of an entire and wrinkled SC sheath in a culture dish after having been extracted from the HA conduit. The cell cylinder is stained with Coomassie brilliant blue R250. (b) Scanning electron microscope image from a longitudinal cut, dividing the HA+SC conduit into two parts, at day 10 of culture. The SC form a continuous sheath coating the inside surface of

the HA conduit's lumen, which presents a smooth surface (arrow), here blue-coloured for the sake of contrast with the material of the conduit's wall, whose porous structure can be clearly seen (stars). (c) Transmission electron microscope image from a transversal section of the SC sheath in the HA conduit for the same culture time. Asterisks indicate the different cell layers that form the SC sheath. Scale bar: 100 μm (a, b), 1 μm (c).

3.2. Pre-seeding of hyaluronic acid conduits with Schwann cells improves axonal extension after 21 days culture of dorsal root ganglion explants

The postnatal P3-4 rat DRG explants were cultured for 21 days at one end of the HA conduit without (figure 3(a), 3(c), 3(d)) and with (figure 3(b), 3(e)-3(h)) pre-seeded SC cultured for 10 days in order to study the influence of the SC on the axonal extension from the DRG explant. Groups HA+DRG and HA+SC+DRG showed significant differences in what refers to axon outgrowth. Figure 3(a) and 3(b) are macroscopic images of both kinds of samples, post-fixed with OsO_4 to have the cellular content stained in black for better visual identification. Both samples show the DRG at the ends (indicated with a white arrow), but only the channel of sample HA+SC+DRG appears black-stained. Cells coming from the DRG had not appreciably penetrated the HA conduit in group HA+DRG. This was further verified in longitudinal cuts (figure 3(c)) and with confocal fluorescent images showing the axonal outgrowth immunostained with Tuj 1 in green (figure 3(d), 3(e)). In the group HA+DRG without SC the DRG explant maintained its original rounded shape without axonal growth out of the DRG explant, without showing signs of cytotoxicity, so the axonal extension could not be quantified. In contrast, the group HA+SC+DRG with pre-seeded SC showed an axonal extension (0.66 ± 0.01 mm) in a significant way, though without any preferred directionality (figure 3(e)). A cross-section normal to the lumen's axis of the HA+SC+DRG conduit was analysed by bright field microscopy after toluidine staining

and by TEM (figure 3(f)-3(g)). Figure 3(f) and 3F' show the compact and continuous SC layer resting at the internal surface of the lumen without adhesive contacts to the conduit substrate (SC sheath indicated with an arrow and HA conduit indicated with a star). As previously, the TEM images showed the tight multilayer SC sheath now also in the HA+SC+DGR conduit (figure 3(g)). Figure 3(h) shows that the SC in the HA+SC+DRG sample possess a well-organized cytoskeleton distribution without picnotic nuclear bodies, indicating a good tolerance of the SC to the DRG growth medium after 21 days of culture. In fact, the SC sheath that appeared here is similar to the SC sheath after 10 days of SC culture (figure 2(b)) being continuous and coating the entire lumen, and the transversal section (figure 3(g)) is also like that in a 10-day SC culture with SC growth medium (figure 2(c)).

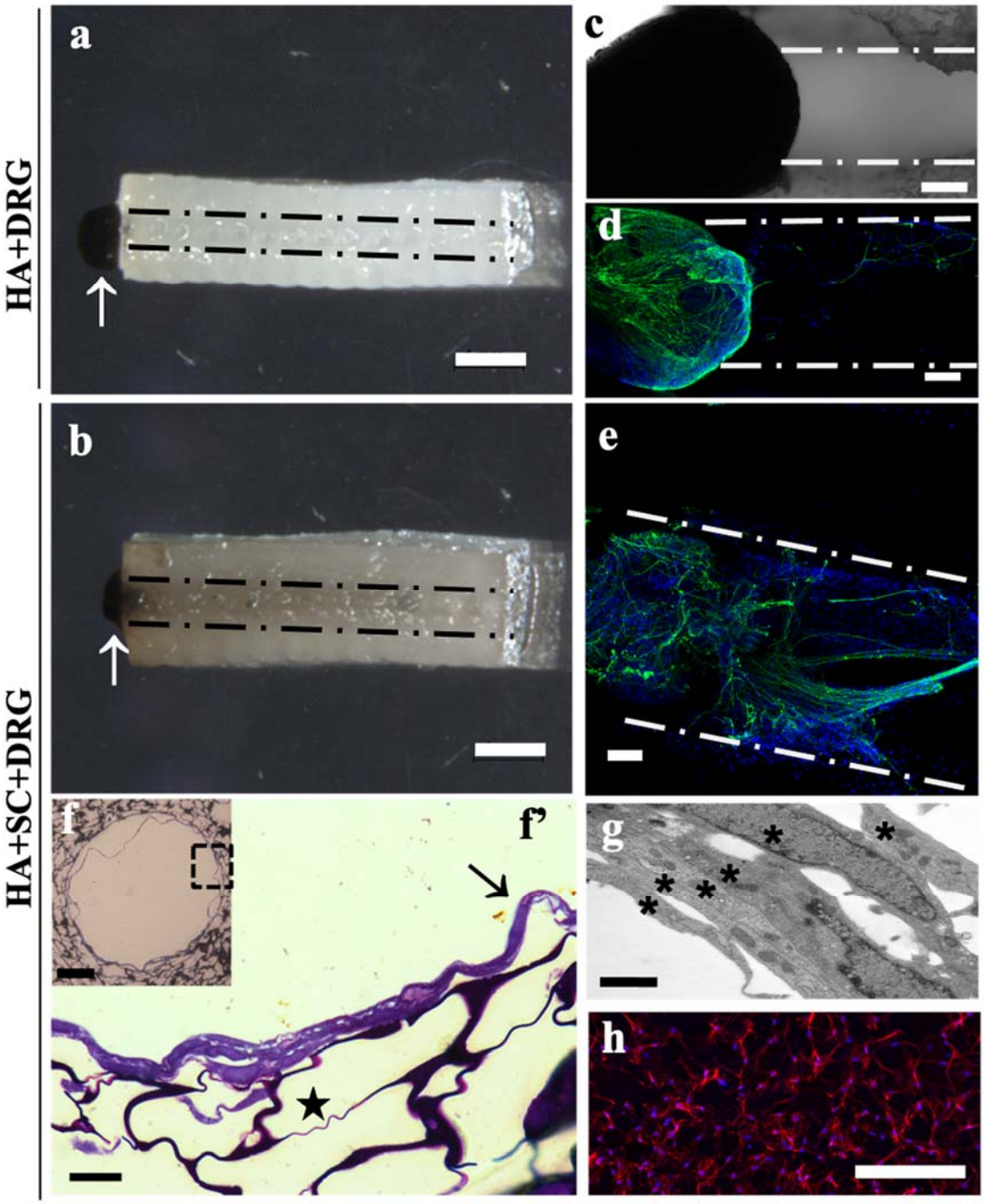

Figure 3. Influence of pre-seeding Schwann cells on cell invasion of the conduit by dorsal root ganglion (DRG) cells after 21-day DRG culture. Macroscopical view of hydrated (a) HA+DRG and (b) HA+SC+DRG conduits and (c) bright-field photograph of a longitudinal section of HA+DRG conduit post-fixed with OsO4 (cells stained in black) showing the DRG explant in one end of the conduit indicated with a white arrow. Confocal fluorescent image showing the longitudinal section of (d) HA+DRG and (e) HA+SC+DRG conduits after nuclear staining with DAPI (blue) and neuronal staining with Tuj 1 (green). (f) Bright field photograph of the transversal section of HA+SC+DRG conduit showing Toluidine blue staining of SC in

the internal lumen of the sample and a detail (f') of the SC sheath (indicated with an arrow). The porous structure of HA is indicated with a star. (g) Transmission electron microscopic image from a transverse section of the SC sheath in the HA+SC+DGR conduit for the same culture time. Asterisks indicate the different layers that form the SC sheath. (h) Confocal fluorescent image of a longitudinal section of HA+SC+DRG after nuclear staining with DAPI (blue) and F-actin of SC staining with ActinRed™ 555 ReadyProbes™ Reagent (red). Dash lines delimit the conduit's lumen: black for samples before the longitudinally cut and white for longitudinal sections (a, b, c, d, e). Scale bar: 1 mm (a, b), 200 µm (h), 100 µm (c, d, e, f), 1 µm (f'), 1 µm (g).

3.3. Schwann cells coat poly-L-lactic acid fibres while still making the sheath-like structure at the hyaluronic acid lumen's inner surface

HAf samples, of HA conduits filled with PLA fibres, were seeded with SC and cultured for 10 days as previously shown. Longitudinal and transversal cuts of these HAf+SC samples were analysed with confocal fluorescent, SEM and TEM microscopies (figure 4). Images of a longitudinal section of HAf+SC after nuclear staining with DAPI and glial staining with S100 in the lumen show that the presence of PLA fibres in the lumen did not hinder the formation of the SC sheath at the conduit's lumen surface (figure 4(a)), being similar to the SC sheath formed in conduits without fibres (figure 2(b)). SC attached to and grew on the PLA fibres too, and completely covered them (figure 4(b), 4(c)). SC on PLA fibres acquired elongated shapes oriented in the direction of the PLA fibre axis (figure 4(c)), which contrasts with the rounded and flattened SC shape that have the cells in the SC sheath (figure 4(a)). The cells coat so densely the fibres, that individual cells connect one PLA fibre to another, making the cell-fibre bundle into an aggregate unit (figure 4(c)). Bright field photograph of the cross-section of HAf+SC conduit (figure 4(d)) shows toluidine blue staining of SC surrounding the PLA fibres and, in detail (figure 4(e)), we could see how SC embrace two PLA fibres (indicated

with *f*). The TEM image of the HAf+SC conduit shows the tight packing of the SC on the fibres' surface (figure 4(f)).

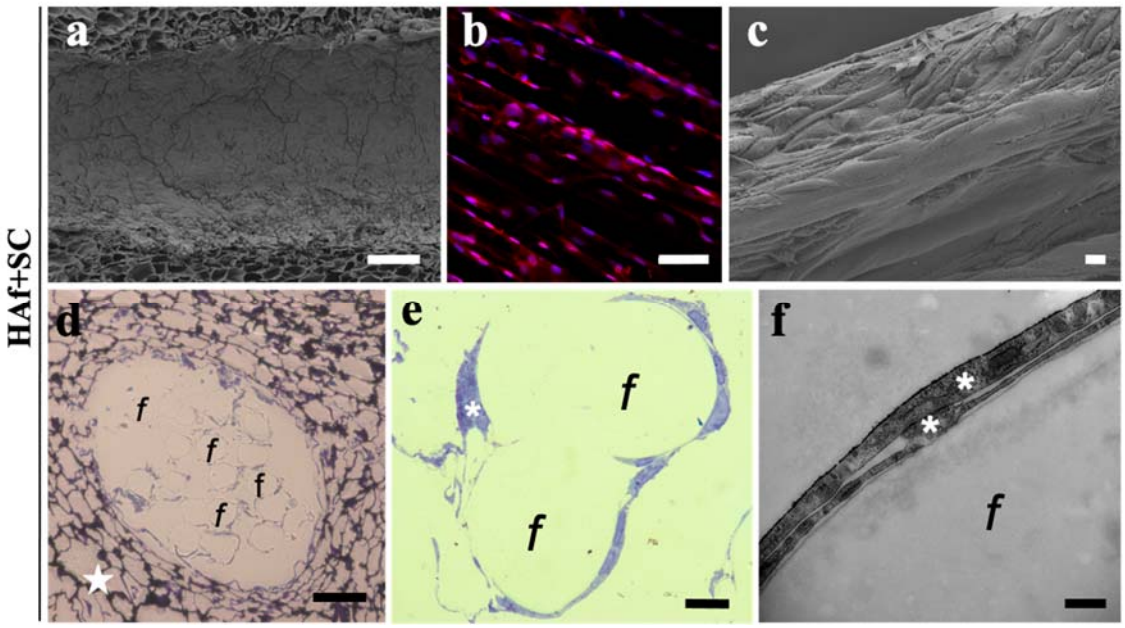

Figure 4. Schwann cells distribution inside the hyaluronic acid conduits with poly-L-lactic acid fibres. Scanning electron microscopic image from a longitudinally cut of the SC tubular sheath in the lumen (a) and PLA fibres (c) of HAf+SC after 10 days of SC culture. (b) Confocal fluorescent images of a longitudinal section of HAf+SC after nuclear staining with DAPI (blue) and glial staining with S100 (red) in PLA fibres for the same culture time. (d) Bright field photograph of the transversal section of HAf+SC conduit showing toluidine blue staining of SC surrounding the PLA fibres and a detail (e) with two fibres. (f) Transmission electron microscopic image from a transverse section of HAf+SC showing SC encircling a PLA fibre. The star indicates the HA, the *f* indicates a PLA fibre and asterisks indicate the different layers of SC. Scale bar: 100 µm (a, d), 50 µm (b), 10 µm (c, e), 500 nm (f).

3. 4. Schwann cells together with poly-L-lactic acid fibres induce directed axon outgrowth from one end to the other of the conduit

DRG explants were cultured for 21 days on one extreme of conduits with (HAf+SC+DRG) and without (HAf+DRG) pre-seeded SC for 10 days, as explained above, to study the influence of aligned PLA fibres on the axonal growth. The DRG

explants attached faster and remained at the end of the conduit more consistently than in the HA group, where it was not infrequent that the explants detached in contact with the culture medium. Macroscopical observation of the entire conduits post-fixed with OsO_4 (cells stained in black) shows higher cell density throughout the lumen of HAf+SC+DRG (figure 5(c)) than in HAf+DRG (figure 5(a)) conduits. Confocal fluorescent reconstructions in figure 5(b) and 5(d), completely spanning the whole length of the PLA fibres after removing the HA conduits, show a nuclear staining with DAPI (blue) and neuronal staining with Tuj 1 (green). The DRG projecting axons fully invade the lumen of the HAf+SC+DRG conduit (figure 5(d)). In the absence of SC (HAf+DRG group), fewer axons were identified (figure 5(b)). A closer look at the fibres of the HAf+SC+DRG constructs shows that the projecting axons stained with Tuj1 (green; figure 5(e)) and the SC stained with p75 (red; figure 5(f)) closely co-exist (figure 5(g)). In the HAf+DRG group, axons elongated through the lumen reaching a length of 1.97 ± 0.82 mm (figure 5(b)), a longer extension than in the HA+DRG (figure 3(c)) and HA+SC+DRG groups (figure 3(h)) groups. The outgrowth found in HAf-DRG group was also more ordered. In the case of the HAf+SC+DRG group, after the 21 days of DRG explant culture, all the analysed specimens showed axons reaching the opposite end of the HA conduit (6 mm) and even exceeding this length growing on the fibres that showed out of the conduit (figure 5(d)). The elongation of axons that could be thus measured reached 7.52 ± 0.71 mm. As fibres protrude at both ends of the HA conduit, axons extended all through the fibres' length, even without the HA enclosure. In the presence of SC, figure 5(d), axonal growth is ordered parallelly on the SC-coated fibres, in the direction of the fibre axis (figure 5(d), 5(e)-5(g)). The SC coating the fibres served as guiding support of the axons all along the whole length.

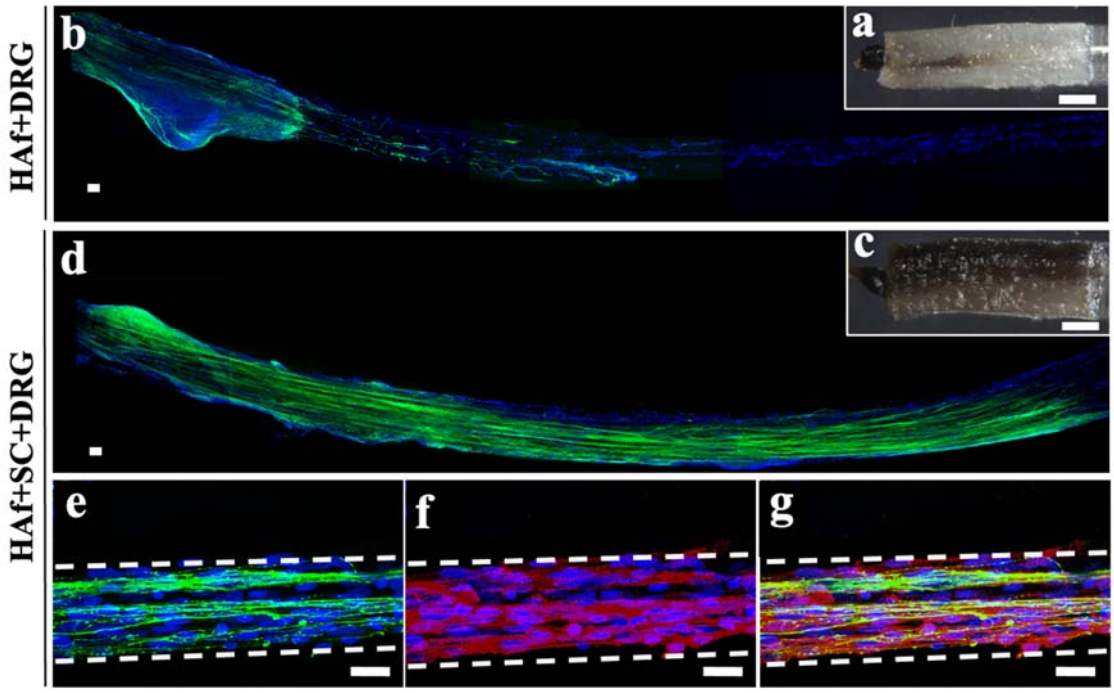

Figure 5. Cell distribution and axon growth in hyaluronic acid conduits with poly-L-lactic acid fibres after 21 days. Macroscopical view of hydrated (a) HAf+DRG and (c) HAf+SC+DRG conduits post-fixed with OsO_4 (cells stained in black) showing the DRG explant at one end of the conduit. Representative confocal reconstruction of the conduit's complete length of (b) HAf+DRG and (d) HAf+SC+DRG conduits, after nuclear staining with DAPI (blue) and neuronal staining with Tuj 1 (green). Confocal fluorescent image of a longitudinal section of HA+SC+DRG after (e) nuclear staining with DAPI and Tuj 1 in green, (f) DAPI and glial marker p75 in red and (g) merge. Dash lines delimit one PLA fibre. Scale bars: 1 mm (a, c), 100 µm (b, d), 20 µm (e, f, g).

GAP43 was employed to trace the active axon outgrowth along the HAf+SC+DRG conduits (figure 6(a) and 6(b); green). The axon growth cones ultrastructure was analysed by TEM. Figure 6(a) shows a confocal reconstruction of the conduit's complete length, made from a series of confocal fluorescent images of longitudinal sections of a HAf+SC+DRG conduit and also a detail (figure 6(b)) for GAP43 immunostaining showing a continuous and abundant staining along the entire axonal projections. We could confirm the presence of growth cones along the entire length

thanks to the TEM images, showing growth cones at the proximal (figure 6(c)) and distal (figure 6(d)) transversal sections of samples. Growth cones (indicated with an asterisk) appeared located between other axons (*Ax*) and glial processes (*SC*) (figure 6(b), 6(c))**.**

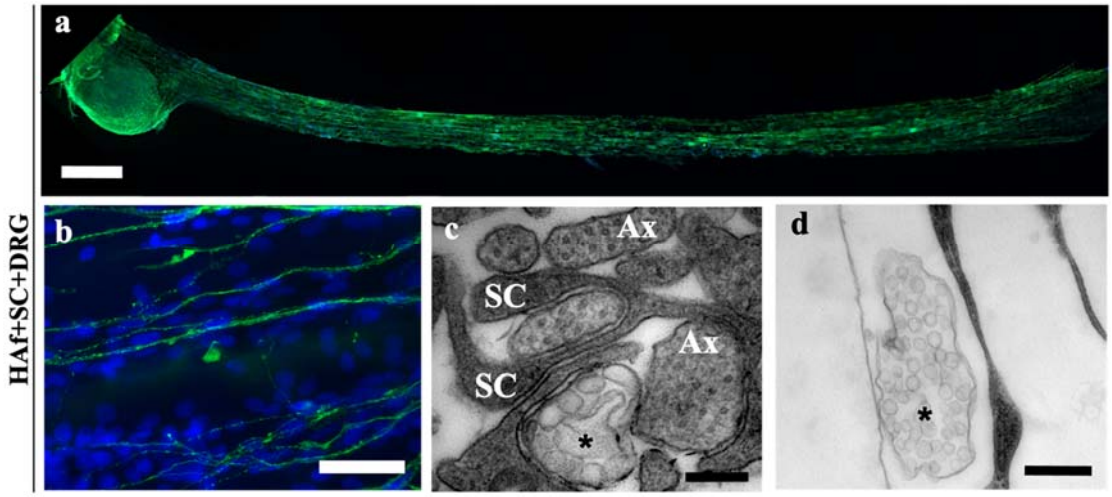

Figure 6. Axonal outgrowth trace in HAf+SC+DRG group. (a) Representative confocal reconstruction of the conduit's complete length of longitudinal sections of HAf+SC+DRG conduit and (b) a detail, after nuclear staining with DAPI (blue) and growth cones staining with GAP43 (green). (c, d) Transmission electron microscopic images from a transverse section of the HAf+SC+DRG conduit showing SC (indicated with *SC*), axons (indicated with *Ax*) and growth cones (indicated with an asterisk). Scale bars: 100 µm (a), 50 µm (b), 500 nm (d), 200 nm (c).

3.5. Different cells from the dorsal root ganglion explant migrate and coexist with the pre-seeded Schwann cells within HAf+SC+DRG

Besides the axon outgrowth from the DRG explants, different cells can migrate from DRG explants such as SC and fibroblast. To identify these, a DRG-GFP explant was used in the experiment. Figure 7 shows that GFP+ cells are present within the HAf+SC+DRG samples after 21 days of DRG explants culture. Red-stained S100+ SC coexist with green-stained GFP+ cells stemming from the explant all along the entire

length of the samples, on the lumen's surface of the conduit and on the PLA fibres (figure 7(a)). TEM images of transversal cuts revealed a large number of cells that appeared to be fibroblasts (marked with an asterisk on figure 7(b)). Fibroblasts appear as thin cells, elongated nuclei and condensed chromatin, with a developed rough endoplasmic reticulum and caveolae. In the direct neighbourhood, many collagen fibres, typically found in these cells, were observed (indicated with arrows on figure 7(b)). Besides fibroblasts, SC migration from the DRG explant into the conduit could also be ascertained by the co-localization of both markers (S100 red and GFP green, giving rise to the yellow colour in the merged image shown in figure 7(a)).

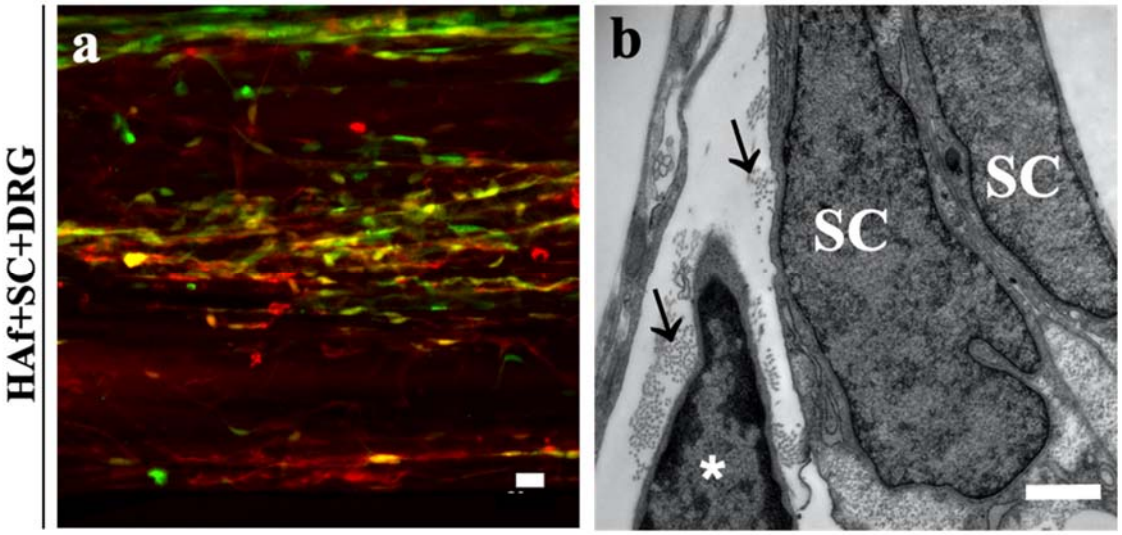

Figure 7. Coexistence of pre-seeded Schwann cells and dorsal root ganglion-GFP explant cells in HAf+SC+DRG group after 21 days. (a) Confocal fluorescent image of a longitudinal section of HAf+SC+DRG conduit, after immunostaining showing S100 glial marker (red) and DRG-GFP explants cells (green). (b) Transmission electron microscopic image from a transverse section of the HAf+SC+DRG conduit showing fibroblast. An asterisk indicates fibroblast and arrows indicate collagen fibres. Scale bar: 20µm (a), 1µm (b).

3.6. Ultrastructural analysis of HAf+SC+DRG shows Schwann cells surrounding unmyelinated bundles of well-preserved axons

We performed an ultrastructural analysis to gain a general sight of the distribution and interaction of the cells inside the HAf+SC+DRG samples after 21 days of DRG explants culture. Figure 8(a) presents a sketch of the sections analysed in TEM. In all proximal (figure 8(b)), medium (figure 8(c)), and distal (figure 8(d)) sections SC could be found surrounding a number of unmyelinated bundles of well-preserved axons. The cross-sections of the axons had the expected cytoplasmic contents of microtubules and neurofilaments), as can be seen in figure 8(e). Also, SC had the normal morphology and structure seen in other *in vitro* studies [47]. Some SC enclosed scattered single axons (figure 8(e)). In some larger bundles, a cytoplasm-rich large SC revealed a complex interaction with the axons by extending several cytoplasmic processes that seemingly subdivided the axon bundle into smaller groups (figure 8(b), 8(c)). All these events were found over the entire length of the conduits. We found that the diameter of the axons was approximately the same along the entire length of the conduit, being <3 μm. Immunostaining for neurites with NF marker (figure 8(h)) and for myelinating SC with MBP marker (figure 8(g)) revealed the association of both cell types again (figure 8(i)). Although the MBP marker is associated with myelinating SC, in the TEM images (figure 8(b)-8(e)) the characteristic structures belonging to the myelin sheath, an electron-dense multi-layered covering around the axons, were not observed. Myelinization in vitro must be induced with different protocols [48,49], so it wasn't expected to occur in our experiments.

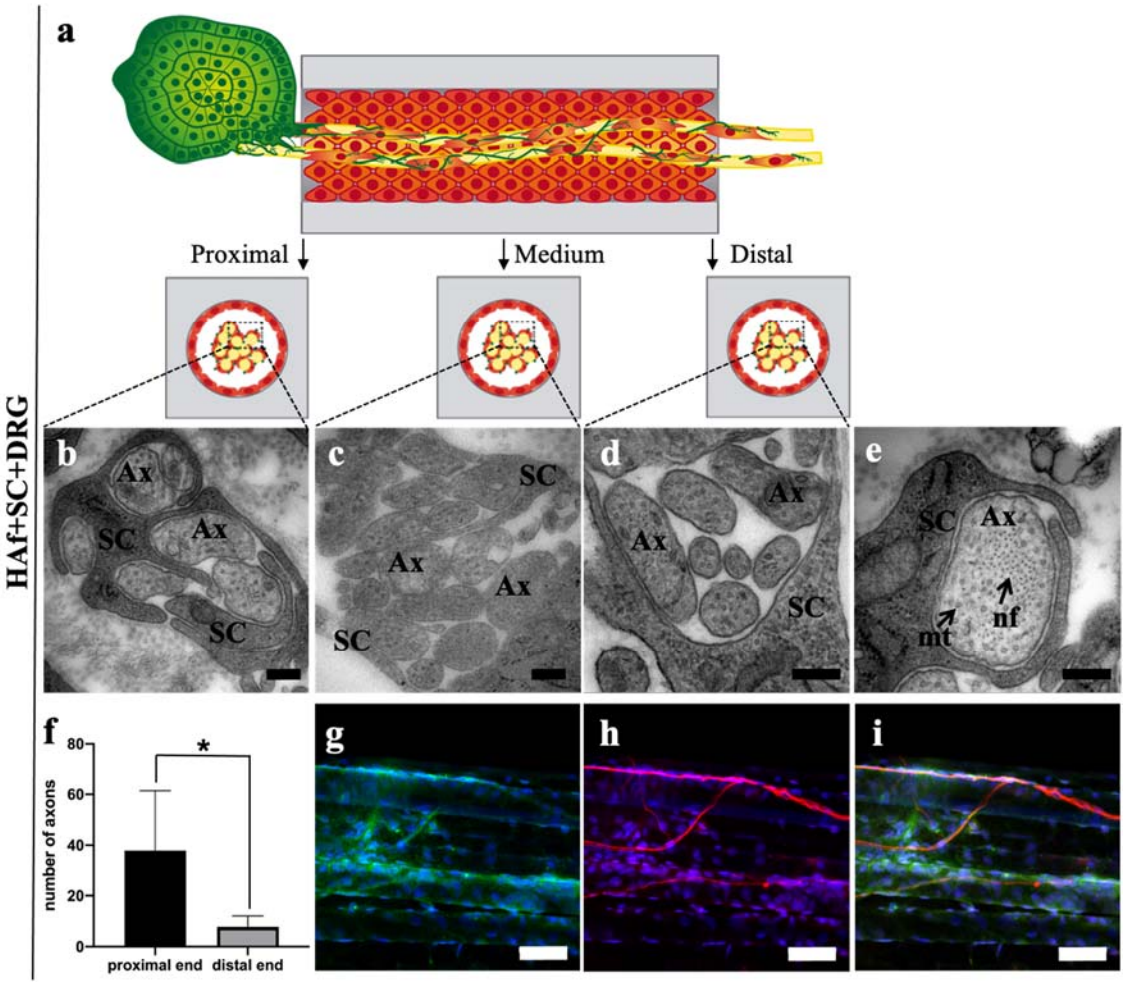

Figure 8. Cell ultrastructure in the HAf+SC+DRG group. (a) Sketch of the locations of the proximal (b), medium (c) and distal (d) cross-sections (normal to conduit axis) taken for transmission electron microscopy (TEM). TEM images of the HAf+SC+DRG conduit at (b) proximal, (c) medium and (d) distal sections. (e) Representative TEM image from a cross-section showing a SC (indicated with *SC*) and an axon (indicated with *Ax*) with its cytoplasmic content of microtubules (indicated with *mt*) and neurofilaments (indicated with *nf*). (f) Quantification of the number of axons at the proximal and distal sections of the conduit. Confocal fluorescent image of a longitudinal section of HAf+SC+DRG after (g) nuclear staining with DAPI in blue and myelinating SC marker MBP in green, (h) DAPI and neurites marker NF in red and (i) merge. Scale bars: 200 nm (a, c, d, e), 50 µm (g, h, i).

4. Discussion

A cells-biomaterials biohybrid construct has been designed to enhance regeneration of axon tracts that mimics *in vitro* aspects of the the *in vivo* physiological situation produced during neural regeneration. Major findings were: 1) The tubular scaffold made by crosslinked HA acts as a template for the development of a SC sheath and can act as a physical shelter in case of cell transplantation, 2) on the PLA fibres the cultured SC form a cover that acts as a directional feeder layer for the axonal extension, 3) the presence of these SC is necessary for a more efficient axon outgrowth, 4) This conjoint association of SC and PLA fibres induces the *in vitro* formation of parallel bundles of SC *plus* axons arrangements that recapitulate the directional features of axon tracts.. These findings prove that both biomaterial cues with different roles and a supportive cell supply are necessary together. Our *in vitro* model, having the neuron somas fixed at one end of the construct, permits an evaluation of the process of directed axonal extension from one fixed point to another distant one. These results may be relevant both for the *in vitro* engineering and the *in vivo* regeneration of axonal pathways in PNS and CNS.

The *in vitro* experimental model keeps the DRG explant at one fixed end of the HA construct. In this way, it allows a study of the kinetics of asymmetric axon growth along the direction supplied by the fibres, in a way that shares some features of physiological situations in which axons outgrowth starts from a spatially fixed neuronal population (proximal neurons in PNS or substantia nigra in the case of the nigrostriatal tract in CNS). We used the DRG explants in the model since they are a source of projecting neurons that we could easily place at a desired specific point, in contrast to other studies where the DRG explants are let to grow in different directions [46,50–52].

The pre-seeded SC cultured for 10 days within the HA conduits developed the sheath-like continuous cell structure (figures 2(b) and 4(a)) on the inner surface of the lumina

previously met in studies [27,28], and grew continuously covering the PLA fibres (figure 4(b), 4(c)). The SC sheath had enough integrity and resisted separate manipulation as a unit, so that it could be easily detached and extracted from the conduit (figure 2(a)). The more elongated shape of the SC on the fibres (figure 4(c)) as compared with their more rounded shape (figure 4(a)) in contact with the HA surface indicates the sensitivity of these cells to the radius of curvature (much greater in the case of the HA lumen surface than in the case of the PLA fibres). Moreover, the formation of these differing types of cellular structures is explained by the highly hydrophilic nature of HA, which allows only for a weak cell adhesion to its surface [53], and the much more cell-adhesive properties of PLA. In this way, the HA conduit acts as a template of the SC sheath but not as an attaching substrate: the HA-SC bond is weaker than the SC-SC bonds, and thus proliferation of the SC leads to an integral one-piece self-assembled SC sheath. In contrast, the SC bind more strongly to the hydrophobic PLA fibres remain adhered on them. PLA fibres, being more hydrophobic, allow the adsorption of ECM proteins [54], and this causes a better adhesion of SC via integrins, generating focal adhesions that promote cell survival. Integrins directly activate survival pathways via the phosphoinositide 3-kinase and mitogen-activated protein kinase pathways [55]. Hence, SC morphology and adhesive response is decisively influenced both by the different HA or PLA chemistries and also by the curvature radius [36].

Moreover, the fact that PLA is adherent favours cell migration compared to other substrates [56]. So, PLA fibres are a physical support for SC, which colonize their span efficiently. The number of PLA fibres placed in the lumen occupy a volume that represents around an 11% of the channel's total volume. This figure is much less that the percentage reported as a inhibiting regeneration within conduits (15-30%) [57]. The SC attached on the PLA fibres associated in an elongated fashion that resembles

microarchitectures such as the Büngner bands formed by SC strands that selectively guide growing axons containing growth-promoting molecules like glycoproteins, laminin and fibronectin [18]. The strategy of creating tubular implants with artificial Büngner bands is something that has been explored previously [58,59], but here we grew SC without any surface functionalization.

The pre-culture of the SC inside the tubular conduit with PLA fibres presents two advantages with regard to the axon growth. Once the DRG are in place, sprouting axons from their neuron somas do encounter an already-made SC feeder layer all along the fibre component of the conduit, and thus do not have to 'wait' for accompaniment in their growth of migrating SC from the DRG itself; as previously pointed out [40,60], SC first migrate and then the axons grow and extend on top of the SC. Second, the pre-seeded SC in high numbers within the lumen space contribute with bioactive factors (like BDNF, NGF, NT-3, GDNF, and VEGF) that are already concentrated in the lumen to be colonized, thanks to the HA conduit.

Although there are studies of axon growth within tubular structures, and also studies employing co-cultures, no study had previously considered this sequential process and its effects on long-term axonal growth inside a tubular conduit with microfibres inside.

Chemotactic stimuli secreted by the SC within the conduit together with the presence of the PLA fibres made axons in HAf+SC+DRG group sprout from the explant, extend along the fibres, and reach the end of the tube with a total axonal extension of 7.52 ± 0.71 mm by the end time of the experiment (21-days) in all specimens (figure 5(d)). So, the differences between HAf+DRG group, where the axonal growth was discrete, and HAf+SC+DRG group must most probably lie in that the growing axons of the HAf+SC+DRG group do not have to wait for SC migrating from the explant, the SC are already there, and the sprouting axons find larger concentrations of neurotrophic factors in the conduit [40,60]. This difference of both experimental groups stresses the

importance of a rich supply of auxiliary cells (here SC) in aiding and potentiating the regeneration possibilities innate naturally in neurons. In contrast to works that employ tubular constructs with a gel filler in the lumen [59,61], our concept critically makes use of both the PLA fibres and the SC. They proved to be effective both in promoting and guiding the axon growth through topographical cues (supplied by the fibres) and biochemical signals contributed by the SC. SC without PLA fibres exerted a positive but discrete effect on axonal growth (experimental group HA+SC+DRG, figure 3(e)). Fibrillar structures have been seen to improve neural regeneration [33,34], and in our work, they lent support to the proliferative capacity of the pre-seeded SC and other cells migrating from the DRG explant [47], and guided their colonization partly thanks to PLA's cell-adhesive properties. This adhesiveness of PLA was advantageous not only for the axonal extension but also for keeping the DRG stably positioned at one end of our constructs at the beginning of the experiments (figure 3(a) and 3(b)).

In humans, axon growth rate during peripheral nerve regeneration can reach 1 mm/day [62], and this rate is significantly reduced in the CNS [63]. DRG axons grow with rates between 130 and 300 μm/day *in vitro* [64]. In the present work, we can estimate the axonal extension rate achieved *in vitro* to lie between 350 and 400 μm/day, a value obtained by dividing the maximum length reached at day 21 by axons through that time. It must be born in mind that this figure represents a lower bound for the actually occurring growth rate since we cannot know whether axons had covered the maximum length of our conduits already before day 21. Considering that the most effective implantable medical devices for functional regeneration currently do not exceed rates of 0.5-1 mm/day [65], our biohybrid construct compares favourably with those types of devices.

Axons growing in our HAf+SC+DRG samples had growing neurites, as evidenced by the appearance of growth cones stained with GAP43 (figure 6). SC aligned in the PLA

fibres could intervene in the extension of the growth cone of the axon pathfinding, which is responsible both for the neuronal circuitry development in the brain [66], and for the regrowth of damage axonal tracts after an injury or disease [67]. It is the growth cone that recognises the molecular cues present in the environment and integrates the information to determine the pathway the growing axon will take by the structural reorganization of the F-actin and microtubules, which modified different intracellular pathways that results in the formation of focal adhesions in the growth cone during axonal extension [68] due to the recognition of cell external adhesion molecules expressed by glial cells such as SC [69]. *In vitro*, DRG adhesion is a prerequisite for neurite extension, and the PLA has demonstrated to serve as a substrate for cells and also ECM proteins [70]. GAP43 is a neuron-specific, membrane-associated phosphoprotein and the most abundant proteins in neuronal growth cones [71]. However, this protein is not confined to neurons but is also expressed by glial cells like SC precursors and in mature non-myelin-forming SC [72]. So, fluorescence images presented here could show these different cell types (figure 6(a), 6(b)). However, it could be confirmed that there are growth cones along the entire length thanks to the TEM images (figure 6(c), 6(d)), similar to other authors results [63].

As previously mentioned, SC surrounded unmyelinated bundles of well-preserved axons (figure 8(b)-8(e)), extending cytoplasmic processes that embraced and subdivided the axon bundles. These axons presented a typical cytoplasmatic content of microtubules (*mt*) and neurofilaments (*nf*). Figure 8(f) shows a rough quantification of the number of axons at the proximal and distal section using TEM images. This quantification is not representative of what happens throughout the section, it should be understood as an approximation, since we have not monitored the intermediate zone of the conduits. Approximately 21% of the axons we count at the beginning of the conduit

reach the end of the 6 mm conduit after 21 days of DRG explant culture, understanding this percentage as extrapolated data from the quantification of TEM images.

SC with myelinic potential were observed thanks to the MBP marker (figure 8(g), 8(i)), although in the TEM images (figure 8(b)-8(e)) the characteristic structures of the myelin sheath were not observed. Probably the absence of myelin was due to the insufficient time in which the experiments are carried out for the myelination process to develop [73]. It could be observed that the neurites were in contact with the SC (figure 5(e)-5(g)) and the way they appeared to extend throughout the cells resembles the neuronal behaviour *in vivo* during regeneration when SC align longitudinally to form the bands of Büngner that regrowing axons use to extend [58]. The ultrastructure of neurites and all the neural tissue developed within the HAf+SC+DRG constructs after 21 days is similar to an unmyelinated nerve *in vivo*, where SC interact with multiple small axons (<3 μm), resulting in non-myelinated nerve fibres formed by axonal bundles surrounded by SC processes [74]. It remains hypothetical whether these structures would evolve towards myelinated structures with a contribution of additional factors and with more time of culture[48]. Altogether, these molecular-biological findings point to a process of axon growth within our conducts that reproduces many features of the natural neural regenerative process, recapitulating hallmarks for axonal pathfinding and cellular organization for axonal tracts regeneration.

The results here presented firmly establish that synergistic effects provided by adhesion and guidance cues of PLA fibres and feeder-like effects of SC grown on them greatly improve the density of axon sprouting and the speed of asymmetrical axon growth from a DRG explant along a desired direction *in vitro*. Future research must study longer distances for axonal regeneration in order to confirm if this combination of PLA fibres and SC confined in a tubular scaffold could overcome the typical limitations of this regeneration.

5. Conclusion

The results obtained suggest that the concept consisting of a tubular conduit of HA with PLA fibres in its interior promotes retention and differential growth of the SC in the two substrates (HA and PLA fibres), allowing a better axonal growth and constitutes a structure that favours the axonal regeneration. The axonal growth takes place directedly, guided by the PLA fibre bundle. This fact allowed the neuron somas placed on one end project their neurites and reach the other end of the tube. The conjoint association of SC and PLA fibres recapitulates directional hallmarks of axonal tracts and induces a more efficient process of axon extension than either SC or PLA fibres per separate. Such structures may represent a step towards the regeneration of injured axonal pathways like nerves in PNS and neural tracts in CNS.

Acknowledgements

The authors acknowledge financing from the Spanish Ministry of Economy and Competitiveness through MINECO grants, Funded by AEI "RTI2018-095872-B-C21 and C22/ERDF", the Valencian Council for Innovation, Universities, Science and Digital Society (PROMETEO/2019/075 to J.M.G-V,) and the Spanish Cell Therapy Network (TerCel-RD16/0011/0026 to J.M.G-V.). Laura Rodríguez Doblado acknowledges scholarship FPU15/04975 of the Spanish Ministry of Education, Culture and Sports. We thank the Microscopy Service at the UPV, where the FESEM images were obtained and Patricia García-Tarraga for her technical support.

Bibliography

[1] C. Aijie, L. Xuan, L. Huimin, Z. Yanli, K. Yiyuan, L. Yuqing, S. Longquan, Nanoscaffolds in promoting regeneration of the peripheral nervous system, Nanomedicine. 13 (2018) 1067–1085. https://doi.org/10.2217/nnm-2017-0389.

[2] T. Manoli, L. Schulz, S. Stahl, P. Jaminet, H.-E. Schaller, Evaluation of Sensory Recovery After Reconstruction of Digital Nerves of the Hand Using Muscle-In-Vein Conduits in Comparison to Nerve Suture or Nerve Autografting, Microsurgery. 34 (2014) 608–15. https://doi.org/10.1002/micr.

[3] M. Curcio, F. Bradke, Axon Regeneration in the Central Nervous System: Facing the Challenges from the Inside, Annu. Rev. Cell Dev. Biol. 34 (2018) 495–521. https://doi.org/10.1146/annurev-cellbio-100617-062508.

[4] S. Ramon y Cajal, Degeneration and Regeneration of the Nervous System, Nature. 125 (1930) 230–231. https://doi.org/10.1038/125230a0.

[5] T. GrandPré, L.I. Shuxin, S.M. Strittmatter, Nogo-66 receptor antagonist peptide promotes axonal regeneration, Nature. 417 (2002) 547–551. https://doi.org/10.1038/417547a.

[6] F. Sun, K.K. Park, S. Belin, D. Wang, T. Lu, G. Chen, K. Zhang, C. Yeung, G. Feng, B.A. Yankner, Z. He, Sustained axon regeneration induced by co-deletion of PTEN and SOCS3, Nature. 480 (2011) 372–375. https://doi.org/10.1038/nature10594.

[7] S. David, A. Aguayo, Axonal elongation into peripheral nervous system "bridges" after central nervous system injury in adult rats, Science (80-.). 214 (1981) 931–933. https://doi.org/10.1126/science.6171034.

[8] I. Espuny-Camacho, K.A. Michelsen, D. Gall, D. Linaro, A. Hasche, J. Bonnefont, C. Bali, D. Orduz, A. Bilheu, A. Herpoel, N. Lambert, N. Gaspard, S. Péron, S.N. Schiffmann, M. Giugliano, A. Gaillard, P. Vanderhaeghen, Pyramidal Neurons Derived from Human Pluripotent Stem Cells Integrate Efficiently into Mouse Brain Circuits In Vivo, Neuron. 77 (2013) 440–456. https://doi.org/10.1016/j.neuron.2012.12.011.

[9] F.I. Jin Y, Bouyer J, Shumsky JS, Haas C, Transplantation of Neural Progenitor Cells in Chronic Spinal Cord Injury, Neuroscience. (2016) 69–82. https://doi.org/10.1016/j.neuroscience.2016.01.066.

[10] C.Z. Chen, B. Neumann, S. Förster, R.J.M. Franklin, Schwann cell remyelination of the central nervous system: Why does it happen and what are the benefits?: Schwann cell remyelination of the CNS, Open Biol. 11 (2021). https://doi.org/10.1098/rsob.200352.

[11] K.D. Anderson, J.D. Guest, W.D. Dietrich, M. Bartlett Bunge, R. Curiel, M. Dididze, B.A. Green, A. Khan, D.D. Pearse, E. Saraf-Lavi, E. Widerström-Noga, P. Wood, A.D. Levi, Safety of Autologous Human Schwann Cell Transplantation in Subacute Thoracic Spinal Cord Injury, J. Neurotrauma. 34 (2017). https://doi.org/10.1089/neu.2016.4895.

[12] H. Saberi, M. Firouzi, Z. Habibi, P. Moshayedi, H.R. Aghayan, B. Arjmand, K. Hosseini, H.E. Razavi, M.S. Yekaninejad, Safety of intramedullary Schwann cell

transplantation for postrehabilitation spinal cord injuries: 2-year follow-up of 33 cases., J. Neurosurg. Spine. 15 (2011) 515–25. https://doi.org/10.3171/2011.6.SPINE10917.

[13] P. Assinck, G.J. Duncan, B.J. Hilton, J.R. Plemel, W. Tetzlaff, Cell transplantation therapy for spinal cord injury, Nat. Neurosci. 20 (2017) 637–647. https://doi.org/10.1038/nn.4541.

[14] H. Kumamaru, P. Lu, E.S. Rosenzweig, K. Kadoya, M.H. Tuszynski, Regenerating Corticospinal Axons Innervate Phenotypically Appropriate Neurons within Neural Stem Cell Grafts, Cell Rep. 26 (2019) 2329-2339.e4. https://doi.org/10.1016/j.celrep.2019.01.099.

[15] P.J. Armati, E.K. Mathey, An update on Schwann cell biology - Immunomodulation, neural regulation and other surprises, J. Neurol. Sci. 333 (2013) 68–72. https://doi.org/10.1016/j.jns.2013.01.018.

[16] K.R. Jessen, Glial cells, Int. J. Biochem. Cell Biol. 36 (2004) 1861–1867. https://doi.org/10.1016/j.biocel.2004.02.023.

[17] G. Nocera, C. Jacob, Mechanisms of Schwann cell plasticity involved in peripheral nerve repair after injury, Cell. Mol. Life Sci. (2020). https://doi.org/10.1007/s00018-020-03516-9.

[18] K.R. Jessen, R. Mirsky, The repair Schwann cell and its function in regenerating nerves, J. Physiol. 594 (2016). https://doi.org/10.1113/JP270874.

[19] L. Chen, H. Huang, H. Xi, F. Zhang, Y. Liu, D. Chen, J. Xiao, A Prospective Randomized Double-Blind Clinical Trial Using a Combination of Olfactory Ensheathing Cells and Schwann Cells for the Treatment of Chronic Complete Spinal Cord Injuries, Cell Transplant. 23 (2014) 35–44. https://doi.org/10.3727/096368914x685014.

[20] M. Georgiou, S.C.J. Bunting, H.A. Davies, A.J. Loughlin, J.P. Golding, J.B. Phillips, Engineered neural tissue for peripheral nerve repair, Biomaterials. 34 (2013) 7335–7343. https://doi.org/10.1016/j.biomaterials.2013.06.025.

[21] L. Ning, H. Sun, T. Lelong, R. Guilloteau, N. Zhu, D.J. Schreyer, X. Chen, 3D bioprinting of scaffolds with living Schwann cells for potential nerve tissue engineering applications, Biofabrication. 10 (2018). https://doi.org/10.1088/1758-5090/aacd30.

[22] Y.S. Lee, S. Wu, T.L. Arinzeh, M.B. Bunge, Transplantation of Schwann Cells Inside PVDF-TrFE Conduits to Bridge Transected Rat Spinal Cord Stumps to Promote Axon Regeneration Across the Gap, J Vis Exp. (2017) 1–7. https://doi.org/10.3791/56077.

[23] J. Bastidas, G. Athauda, G. De La Cruz, W.M. Chan, R. Golshani, Y. Berrocal, M. Henao, A. Lalwani, C. Mannoji, M. Assi, P.A. Otero, A. Khan, A.E. Marcillo, M. Norenberg, A. D. Levi, P.M. Wood, J.D. Guest, W.D. Dietrich, M. Bartlett Bunge, D.D. Pearse, Human Schwann cells exhibit long-term cell survival, are not tumorigenic and promote repair when transplanted into the contused spinal cord, Glia. 65 (2017) 1278–1301. https://doi.org/10.1002/glia.23161.

[24] L.A. Struzyna, K. Katiyar, D.K. Cullen, Living scaffolds for neuroregeneration,

Curr. Opin. Solid State Mater. Sci. 18 (2014) 308–318. https://doi.org/10.1016/j.cossms.2014.07.004.

[25] S. Vijayavenkataraman, Nerve guide conduits for peripheral nerve injury repair: A review on design, materials and fabrication methods, Acta Biomater. 106 (2020) 54–69. https://doi.org/10.1016/j.actbio.2020.02.003.

[26] R.E. Thompson, J. Pardieck, L. Smith, P. Kenny, L. Crawford, M. Shoichet, S. Sakiyama-Elbert, Effect of hyaluronic acid hydrogels containing astrocyte-derived extracellular matrix and/or V2a interneurons on histologic outcomes following spinal cord injury, Biomaterials. 162 (2018). https://doi.org/10.1016/j.biomaterials.2018.02.013.

[27] G. Vilariño-Feltrer, C. Martínez-Ramos, A. Monleón-De-La-Fuente, A. Vallés-Lluch, D. Moratal, J.A. Barcia Albacar, M. Monleón Pradas, Schwann-cell cylinders grown inside hyaluronic-acid tubular scaffolds with gradient porosity, Acta Biomater. 30 (2016) 199–211. https://doi.org/10.1016/j.actbio.2015.10.040.

[28] I. Ortuño-Lizarán, G. Vilariño-Feltrer, C. Martínez-Ramos, M.M. Pradas, A. Vallés-Lluch, Influence of synthesis parameters on hyaluronic acid hydrogels intended as nerve conduits, Biofabrication. 8 (2016) 045011. https://doi.org/10.1088/1758-5090/8/4/045011.

[29] Y. Liang, P. Walczak, J.W.M. Bulte, The survival of engrafted neural stem cells within hyaluronic acid hydrogels, Biomaterials. 34 (2013) 5521–5529. https://doi.org/10.1016/j.biomaterials.2013.03.095.

[30] S.K. Seidlits, Z.Z. Khaing, R.R. Petersen, J.D. Nickels, J.E. Vanscoy, J.B. Shear, C.E. Schmidt, The effects of hyaluronic acid hydrogels with tunable mechanical properties on neural progenitor cell differentiation, Biomaterials. 31 (2010) 3930–3940. https://doi.org/10.1016/j.biomaterials.2010.01.125.

[31] M. Salehi, M. Naseri-Nosar, S. Ebrahimi-Barough, M. Nourani, A. Khojasteh, A.A. Hamidieh, A. Amani, S. Farzamfar, J. Ai, Sciatic nerve regeneration by transplantation of Schwann cells via erythropoietin controlled-releasing polylactic acid/multiwalled carbon nanotubes/gelatin nanofibrils neural guidance conduit, J. Biomed. Mater. Res. - Part B Appl. Biomater. 106 (2018) 1463–1476. https://doi.org/10.1002/jbm.b.33952.

[32] M.C. Araque-Monrós, A. Vidaurre, L. Gil-Santos, S. Gironés Bernabé, M. Monleón-Pradas, J. Más-Estellés, Study of the degradation of a new PLA braided biomaterial in buffer phosphate saline, basic and acid media, intended for the regeneration of tendons and ligaments, Polym. Degrad. Stab. 98 (2013) 1563–1570. https://doi.org/10.1016/j.polymdegradstab.2013.06.031.

[33] D. Li, X. Pan, B. Sun, T. Wu, W. Chen, C. Huang, Q. Ke, H.A. Ei-Hamshary, S.S. Al-Deyab, X. Mo, Nerve conduits constructed by electrospun P(LLA-CL) nanofibers and PLLA nanofiber yarns, J. Mater. Chem. B. 3 (2015) 8823–8831. https://doi.org/10.1039/c5tb01402f.

[34] S.W. Peng, C.W. Li, I.M. Chiu, G.J. Wang, Nerve guidance conduit with a hybrid structure of a PLGA microfibrous bundle wrapped in a micro/nanostructured membrane, Int. J. Nanomedicine. 12 (2017) 421–432. https://doi.org/10.2147/IJN.S122017.

[35] C. Martínez-Ramos, L.R. Doblado, E.L. Mocholi, A. Alastrue-Agudo, M.S. Petidier, E. Giraldo, M.M. Pradas, V. Moreno-Manzano, Biohybrids for spinal cord injury repair, J. Tissue Eng. Regen. Med. 13 (2019) 509–521. https://doi.org/10.1002/term.2816.

[36] R.M. Smeal, R. Rabbitt, R. Biran, P.A. Tresco, Substrate curvature influences the direction of nerve outgrowth, Ann. Biomed. Eng. 33 (2005) 376–382. https://doi.org/10.1007/s10439-005-1740-z.

[37] R. Li, D. Li, C. Wu, L. Ye, Y. Wu, Y. Yuan, S. Yang, L. Xie, Y. Mao, T. Jiang, Y. Li, J. Wang, H. Zhang, X. Li, J. Xiao, Nerve growth factor activates autophagy in Schwann cells to enhance myelin debris clearance and to expedite nerve regeneration, Theranostics. 10 (2020) 1649–1677. https://doi.org/10.7150/thno.40919.

[38] S. Yi, Q.H. Wang, L.L. Zhao, J. Qin, Y.X. Wang, B. Yu, S.L. Zhou, MiR-30c promotes Schwann cell remyelination following peripheral nerve injury, Neural Regen. Res. 12 (2017) 1708–1714. https://doi.org/10.4103/1673-5374.217351.

[39] G. Chen, X. Luo, W. Wang, Y. Wang, F. Zhu, W. Wang, Interleukin-1β promotes schwann cells de-differentiation in wallerian degeneration via the c-JUN/AP-1 pathway, Front. Cell. Neurosci. 13 (2019) 1–10. https://doi.org/10.3389/fncel.2019.00304.

[40] E. Schnell, K. Klinkhammer, S. Balzer, G. Brook, D. Klee, P. Dalton, J. Mey, Guidance of glial cell migration and axonal growth on electrospun nanofibers of poly-ε-caprolactone and a collagen/poly-ε-caprolactone blend, Biomaterials. 28 (2007) 3012–3025. https://doi.org/10.1016/j.biomaterials.2007.03.009.

[41] J.A. Gomez-Sanchez, C. Gomis-Coloma, C. Morenilla-Palao, G. Peiro, E. Serra, M. Serrano, H. Cabedo, Epigenetic induction of the Ink4a/Arf locus prevents Schwann cell overproliferation during nerve regeneration and after tumorigenic challenge, Brain. 136 (2013) 2262–2278. https://doi.org/10.1093/brain/awt130.

[42] A. Vaquié, A. Sauvain, M. Duman, G. Nocera, B. Egger, F. Meyenhofer, L. Falquet, L. Bartesaghi, R. Chrast, C.M. Lamy, S. Bang, S.R. Lee, N.L. Jeon, S. Ruff, C. Jacob, Injured Axons Instruct Schwann Cells to Build Constricting Actin Spheres to Accelerate Axonal Disintegration, Cell Rep. 27 (2019) 3152-3166.e7. https://doi.org/10.1016/j.celrep.2019.05.060.

[43] K. Xi, Y. Gu, J. Tang, H. Chen, Y. Xu, L. Wu, F. Cai, L. Deng, H. Yang, Q. Shi, W. Cui, L. Chen, Microenvironment-responsive immunoregulatory electrospun fibers for promoting nerve function recovery, Nat. Commun. 11 (2020). https://doi.org/10.1038/s41467-020-18265-3.

[44] A.H. Teuschl, C. Schuh, R. Halbweis, K. Pajer, G. Márton, R. Hopf, S. Mosia, D. Rünzler, H. Redl, A. Nógrádi, T. Hausner, A New Preparation Method for Anisotropic Silk Fibroin Nerve Guidance Conduits and Its Evaluation in Vitro and in a Rat Sciatic Nerve Defect Model, Tissue Eng. - Part C Methods. 21 (2015) 945–957. https://doi.org/10.1089/ten.tec.2014.0606.

[45] X. Chen, Y. Zhao, X. Li, Z. Xiao, Y. Yao, Y. Chu, B. Farkas, I. Romano, F. Brandi, J. Dai, Functional Multichannel Poly(Propylene Fumarate)-Collagen Scaffold with Collagen-Binding Neurotrophic Factor 3 Promotes Neural Regeneration After Transected Spinal Cord Injury, Adv. Healthc. Mater. 7 (2018)

1–13. https://doi.org/10.1002/adhm.201800315.

[46] F. Gisbert Roca, J. Más Estellés, M. Monleón Pradas, C. Martínez-Ramos, Axonal extension from dorsal root ganglia on fibrillar and highly aligned poly(lactic acid)-polypyrrole substrates obtained by two different techniques: Electrospun nanofibres and extruded microfibres, Int. J. Biol. Macromol. 163 (2020) 1959–1969. https://doi.org/10.1016/j.ijbiomac.2020.09.181.

[47] R. Bunge, Tissue culture observations relevant to the study of axon-Schwann cell interactions during peripheral nerve development and repair, J Exp Biol. 132 (1987) 21–34.

[48] N. Callizot, M. Combes, R. Steinschneider, P. Poindron, A new long term in vitro model of myelination, Exp. Cell Res. 317 (2011) 2374–2383. https://doi.org/10.1016/j.yexcr.2011.07.002.

[49] C. Taveggia, A. Bolino, DRG Neuron/Schwann Cells Myelinating Cocultures, in: Woodhoo A. Myelin. Methods Mol. Biol., 2018: pp. 115–129. https://doi.org/10.1007/978-1-4939-7862-5_9.

[50] H.B. Wang, M.E. Mullins, J.M. Cregg, C.W. McCarthy, R.J. Gilbert, Varying the diameter of aligned electrospun fibers alters neurite outgrowth and Schwann cell migration, Acta Biomater. 6 (2010) 2970–2978. https://doi.org/10.1016/j.actbio.2010.02.020.

[51] D.L. Puhl, J.L. Funnell, A.R. D'Amato, J. Bao, D. V. Zagorevski, Y. Pressman, D. Morone, A.E. Haggerty, M. Oudega, R.J. Gilbert, Aligned Fingolimod-Releasing Electrospun Fibers Increase Dorsal Root Ganglia Neurite Extension and Decrease Schwann Cell Expression of Promyelinating Factors, Front. Bioeng. Biotechnol. 8 (2020) 1–18. https://doi.org/10.3389/fbioe.2020.00937.

[52] A.R. D'Amato, D.L. Puhl, A.M. Ziemba, C.D.L. Johnson, J. Doedee, J. Bao, R.J. Gilbert, Exploring the effects of electrospun fiber surface nanotopography on neurite outgrowth and branching in neuron cultures, PLoS One. 14 (2019) 1–18. https://doi.org/10.1371/journal.pone.0211731.

[53] M. Arnal-Pastor, C. Martínez Ramos, M. Pérez Garnés, M. Monleón Pradas, A. Vallés Lluch, Electrospun adherent-antiadherent bilayered membranes based on cross-linked hyaluronic acid for advanced tissue engineering applications, Mater. Sci. Eng. C. 33 (2013) 4086–4093. https://doi.org/10.1016/j.msec.2013.05.058.

[54] J.C. Rodríguez Hernández, M.S. Sánchez, J.M. Soria, J.L. Gómez Ribelles, M.M. Pradas, Substrate chemistry-dependent conformations of single laminin molecules on polymer surfaces are revealed by the phase signal of atomic force microscopy, Biophys. J. 93 (2007) 202–207. https://doi.org/10.1529/biophysj.106.102491.

[55] D.G. Stupack, D.A. Cheresh, Get a ligand, get a life: Integrins, signaling and cell survival, J. Cell Sci. 115 (2002) 3729–3738. https://doi.org/10.1242/jcs.00071.

[56] T. Witko, D. Solarz, K. Feliksiak, K. Haraźna, Z. Rajfur, M. Guzik, Insights into In Vitro Wound Closure on Two Biopolyesters—Polylactide and Polyhydroxyoctanoate, Materials (Basel). 13 (2020) 2793. https://doi.org/10.3390/ma13122793.

[57] T.T.B. Ngo, P.J. Waggoner, A.A. Romero, K.D. Nelson, R.C. Eberhart, G.M. Smith, Poly(L-lactide) microfilaments enhance peripheral nerve regeneration across extended nerve lesions, J. Neurosci. Res. 72 (2003) 227–238. https://doi.org/10.1002/jnr.10570.

[58] V.T. Ribeiro-Resende, B. Koenig, S. Nichterwitz, S. Oberhoffner, B. Schlosshauer, Strategies for inducing the formation of bands of Büngner in peripheral nerve regeneration, Biomaterials. 30 (2009) 5251–5259. https://doi.org/10.1016/j.biomaterials.2009.07.007.

[59] K. V. Panzer, J.C. Burrell, K.V.T. Helm, E.M. Purvis, Q. Zhang, A.D. Le, J.C. O'Donnell, D.K. Cullen, Tissue Engineered Bands of Büngner for Accelerated Motor and Sensory Axonal Outgrowth, Front. Bioeng. Biotechnol. 8 (2020) 1–19. https://doi.org/10.3389/fbioe.2020.580654.

[60] Y. tae Kim, V.K. Haftel, S. Kumar, R. V. Bellamkonda, The role of aligned polymer fiber-based constructs in the bridging of long peripheral nerve gaps, Biomaterials. 29 (2008) 3117–3127. https://doi.org/10.1016/j.biomaterials.2008.03.042.

[61] D.K. Cullen, M.D. Tang-Schomer, L.A. Struzyna, A.R. Patel, V.E. Johnson, J.A. Wolf, D.H. Smith, Microtissue engineered constructs with living axons for targeted nervous system reconstruction., Tissue Eng. Part A. 18 (2012) 2280–9. https://doi.org/10.1089/ten.TEA.2011.0534.

[62] H.J. Seddon, P.B. Medawar, H. Smith, Rate of regeneration of peripheral nerves in man, J. Physiol. 102 (1943) 191–215. https://doi.org/10.1113/jphysiol.1943.sp004027.

[63] D.J. Schreyer, E.G. Jones, Growth and target finding by axons of the corticospinal tract in prenatal and postnatal rats, Neuroscience. 7 (1982) 1837–1853. https://doi.org/10.1016/0306-4522(82)90001-X.

[64] A.P. Balgude, X. Yu, A. Szymanski, R. V. Bellamkonda, Agarose gel stiffness determines rate of DRG neurite extension in 3D cultures, Biomaterials. 22 (2001) 1077–1084. https://doi.org/10.1016/S0142-9612(00)00350-1.

[65] T. Nakamura, Y. Inada, S. Fukuda, M. Yoshitani, A. Nakada, S.I. Itoi, S.I. Kanemaru, K. Endo, Y. Shimizu, Experimental study on the regeneration of peripheral nerve gaps through a polyglycolic acid-collagen (PGA-collagen) tube, Brain Res. 1027 (2004) 18–29. https://doi.org/10.1016/j.brainres.2004.08.040.

[66] M. O'Donnell, R.K. Chance, G.J. Bashaw, Axon Growth and Guidance: Receptor Regulation and Signal Transduction, Physiol. Behav. 32 (2009) 383–412. https://doi.org/10.1146/annurev.neuro.051508.135614.Axon.

[67] R.R. Bernhardt, Cellular and molecular bases of axonal regeneration in the fish central nervous system, Exp. Neurol. 157 (1999) 223–240. https://doi.org/10.1006/exnr.1999.7059.

[68] K. Kalil, E.W. Dent, Touch and go: Guidance cues signal to the growth cone cytoskeleton, Curr. Opin. Neurobiol. 15 (2005) 521–526. https://doi.org/10.1016/j.conb.2005.08.005.

[69] E. Tamariz, A. Varela-Echavarría, The discovery of the growth cone and its

influence on the study of axon guidance, Front. Neuroanat. 9 (2015) 1–9. https://doi.org/10.3389/fnana.2015.00051.

[70] R.J. Wade, J.A. Burdick, Engineering ECM signals into biomaterials, Mater. Today. 15 (2012) 454–459. https://doi.org/10.1016/S1369-7021(12)70197-9.

[71] J.H.P. Skene, R.D. Jacobson, G.J. Snipes, C.B. McGuire, J.J. Norden, J.A. Freeman, A protein induced during nerve growth (GAP-43) is a major component of growth-cone membranes, Science (80-.). 233 (1986) 783–786. https://doi.org/10.1126/science.3738509.

[72] Z. Liu, Y.Q. Jin, L. Chen, Y. Wang, X. Yang, J. Cheng, W. Wu, Z. Qi, Z. Shen, Specific marker expression and cell state of Schwann cells during culture in vitro, PLoS One. 10 (2015) 1–17. https://doi.org/10.1371/journal.pone.0123278.

[73] X. Luo, M. Prior, W. He, X. Hu, X. Tang, W. Shen, S. Yadav, S. Kiryu-Seo, R. Miller, B.D. Trapp, R. Yan, Cleavage of neuregulin-1 by BACE1 or ADAM10 protein produces differential effects on myelination, J. Biol. Chem. 286 (2011) 23967–23974. https://doi.org/10.1074/jbc.M111.251538.

[74] R. King, Microscopic anatomy: Normal structure, 1st ed., Elsevier B.V., 2013. https://doi.org/10.1016/B978-0-444-52902-2.00002-3.